

1 **Biochemical and Genetic Evidence Supports Fyv6 as a Second-Step Splicing Factor in**
2 ***Saccharomyces cerevisiae***

3 Karli A. Lipinski^{1,*}, Katherine A. Senn^{2,*}, Natalie J. Zeps², Aaron A. Hoskins^{1,2,†}

4

5 ¹Department of Chemistry, University of Wisconsin-Madison, Madison, WI 53706

6 ²Department of Biochemistry, University of Wisconsin-Madison, Madison, WI 53706

7 *These authors contributed equally to this work

8 †**CORRESPONDING AUTHOR:**

9 Aaron A. Hoskins, ahoskins@wisc.edu

10

11 **RUNNING TITLE:** Fyv6 is a yeast splicing factor

12 **KEYWORDS:** Fyv6, FAM192A, spliceosome, yeast, RNA splicing

13 **ABSTRACT**

14 Precursor mRNA (pre-mRNA) splicing is an essential process for gene expression in
15 eukaryotes catalyzed by the spliceosome in two transesterification steps. The spliceosome is a
16 large, highly dynamic complex composed of 5 small nuclear RNAs and dozens of proteins, some
17 of which are needed throughout the splicing reaction while others only act during specific stages.
18 The human protein FAM192A was recently proposed to be a splicing factor that functions during
19 the second transesterification step, exon ligation, based on analysis of cryo-electron microscopy
20 (cryo-EM) density. It was also proposed that Fyv6 might be the functional *S. cerevisiae* homolog
21 of FAM192A; however, no biochemical or genetic data has been reported to support this
22 hypothesis. Herein, we show that Fyv6 is a splicing factor and acts during exon ligation. Deletion
23 of *FYV6* results in genetic interactions with the essential splicing factors Prp8, Prp16, and Prp22;
24 decreases splicing *in vivo* of reporter genes harboring intron substitutions that limit the rate of
25 exon ligation; and changes 3' splice site (SS) selection. Together, these data suggest that Fyv6
26 is a component of the spliceosome and the potential functional and structural homolog of human
27 FAM192A.

28 INTRODUCTION

29 The removal of introns from pre-mRNA molecules is carried out by the spliceosome, a
30 large macromolecular complex made up of five small nuclear RNAs (snRNAs) and dozens of
31 proteins which assemble de novo on each pre-mRNA substrate. Splicing consists of two, stepwise
32 transesterification reactions in which the 5' splice site (the boundary between the 5' exon and the
33 intron; 5' SS) is first cleaved by formation of a lariat intron and then the intron is released
34 concomitant with exon ligation by attack of the 5' exon at the 3' SS. Spliceosome composition
35 changes dramatically throughout the course of splicing due to the sequential arrivals and
36 departures of different components as well as large-scale conformational changes (Plaschka, et
37 al., 2019). This results in the formation of several intermediate complexes with distinct
38 architectures during the reaction, many of which have now been visualized by cryo-electron
39 microscopy (cryo-EM) (Plaschka et al., 2019). Cleavage of the 5' SS is completed during the
40 transition from the spliceosome B* to the C complex, and exon ligation occurs during the transition
41 between the C* and P (product) complexes. While some components of the spliceosome remain
42 part of the machine throughout the reaction, others transiently associate, dissociate, or re-arrange
43 to interact with the catalytic site only at specific times. Just prior to 5' SS cleavage, the 1st step
44 factors (Cwc25, Isy1, and Yju2) function to juxtapose the 5' SS and branch site (BS) (Wan et al.,
45 2019; Liu Y-C et al., 2007; Villa and Guthrie, 2005; Chiu et al., 2009; Wilkinson et al., 2021).
46 Cwc25, Isy1, and Yju2 are then released after 5' SS cleavage, and 2nd step factors bind (Slu7,
47 Prp18) or are repositioned (Prp17) to facilitate exon ligation (Plaschka et al., 2019; James et al.,
48 2002; Yan et al., 2017; Fica et al., 2017; Ohrt et al., 2013; Tseng et al. 2011). Proper progression
49 through splicing requires the coordinated association and dissociation of these 1st and 2nd step
50 factors with the active site and these transitions are enabled, in part, by ATP-dependent DExD/H-
51 box helicases. The ATPase Prp16 promotes rearrangement of the spliceosome active site and
52 splicing factor release between the 1st and 2nd step of splicing (Schwer and Guthrie, 1992; Semlow

53 et al., 2016), while Prp22 promotes release of the mRNA product from the spliceosome after exon
54 ligation (Wagner et al., 1998; Schwer, 2008).

55 Recently, a putative new 2nd step factor (FAM192A or PIP30) was identified for the human
56 spliceosome. The protein was found by fitting unassigned density present in cryo-EM maps of
57 spliceosomes transitioning between conformations competent for the 1st and 2nd steps (Zhan et
58 al., 2022). Depletion of FAM192A from human nuclear extracts reduced *in vitro* splicing but adding
59 purified protein back did not restore this activity, potentially due to simultaneous depletion of other,
60 unidentified splicing factors (Zhan et al., 2022). Consequently, its role in splicing is still poorly
61 defined.

62 Interestingly, Zhan et al. also identified a potential FAM192A homolog, Fyv6 (Function
63 required for yeast viability 6), in *Saccharomyces cerevisiae* (hereafter, yeast) despite having less
64 than 20% sequence identity (**Fig. 1A**). (It should be noted, however, that this level of sequence
65 identity is similar to that between yeast and human homologs of the other 2nd-step factors Slu7
66 and Prp18). The predicted AlphaFold structure of Fyv6 (Jumper et al., 2021) was able to be
67 modeled into unassigned EM density from yeast C* spliceosome complexes (previously labeled
68 as unknown protein X) (Zhan et al., 2022) (**Fig. 1B**). Prior to this work, Fyv6 had been detected
69 by mass spectrometry analysis of purified B^{act} and C complex spliceosomes (Warkocki et al.,
70 2009; Fabrizio et al., 2009) as well as postulated to be responsible for unassigned density in a
71 cryo-EM structure of a yeast P complex spliceosome (referred to as UNK in that structure, **Fig.**
72 **1C**) (Liu et al., 2017). In both the C* and P complex spliceosomes, the unassigned EM density is
73 located in a position that could significantly impact splicing chemistry: in C* the density contacts
74 core splicing factors Cef1, Syf1, and Prp8 while in P complex it contacts these factors in addition
75 to the lariat intron, Slu7, and Prp22 (**Figs. 1, S1**). Together the combined cryo-EM and mass
76 spectrometry data hint at Fyv6 functioning during splicing; however, no genetic or biochemical
77 evidence for this has been reported.

78 Fyv6 is a poorly studied and nonessential yeast protein originally identified in a screen for
79 mutants sensitive to K1 killer toxin (Pagé et al., 2003). Since identification, Fyv6 has appeared in
80 genetic screens for mutants with sensitivity to heat (Auesukaree et al., 2002), calcineurin inhibitor
81 FK506 (Viladevall et al., 2004), and changes to cell size (Maitra et al., 2019). Fyv6 is localized to
82 the nucleus and has previously been proposed to play a role in nonhomologous end joining, but
83 little is known about its function or interacting partners (Huh et al., 2003; Wilson, 2002). Here, we
84 studied the function of Fyv6 during splicing by probing genetic interactions between Fyv6 and the
85 splicing factors Prp8, Prp16, and Prp22. In addition, we assayed its impact on splicing *in vivo* by
86 deleting *FYV6* and with use of ACT1-CUP1 splicing reporters. Together, these data are consistent
87 with Fyv6 functioning as a 2nd-step splicing factor in yeast.

88 RESULTS AND DISCUSSION

89 Genetic Interactions between Fyv6 and Prp8 1st or 2nd-Step Alleles

90 To examine a potential role for Fyv6 in splicing, we deleted *FYV6* from the yeast genome,
91 confirmed the deletion by PCR (**Fig. S2**), and assayed for genetic interactions with known splicing
92 factors. While *FYV6* is nonessential for yeast viability, its deletion does cause a slow growth defect
93 at 30°C and both cold and temperature sensitivity (*cs* and *ts*) phenotypes at other temperatures
94 (**Fig 1D**). We first tested for genetic interactions with the essential spliceosome component Prp8.
95 Prp8 is a central protein in the spliceosome that scaffolds the active site RNAs and can impact
96 equilibria between the intron branching and exon ligation reactions through structural
97 rearrangement (Query and Konarska, 2004; Fica and Nagai, 2017). As such, multiple alleles of
98 Prp8 stabilize the spliceosome in either the 1st or 2nd-step conformation at the expense of the
99 other state (**Fig. 2A**) (Umen and Guthrie, 1995a; Schneider et al., 2004; Query and Konarska,
100 2004; Liu L. et al., 2007). Moreover, alleles of 2nd step factors Prp18 and Slu7 (*prp18-1*, *slu7-1*,
101 *slu7-ccss*) are synthetically lethal with a 1st step allele of Prp8 (*prp8-101* or Prp8^{E1960K}; Umen and
102 Guthrie, 1995b), presumably since both alleles work in concert to promote the 1st step or inhibit
103 proper progression to the 2nd step. Since Fyv6, like Slu7 and Prp18, is predicted to interact with

104 Prp8 (**Fig. S1**), we expected that genetic interactions should occur between Fyv6 and Prp8 if the
105 former is also involved in splicing.

106 Plasmid shuffle of a gene expressing Prp8^{E1960K} into a *fyv6Δ* strain resulted in synthetic
107 lethality even at the normally permissive temperature of 30°C (**Fig. 2B**). Synthetic lethality was
108 also observed for another 1st-step allele of Prp8, *prp8-R1753K* (**Fig. 2B**). In contrast, when we
109 shuffled in a 2nd-step allele, *prp8-161* (Prp8^{P986T}), we observed suppression of the growth defect
110 caused by *fyv6Δ* at both 30 and 37°C (**Figs. 2B, C**). When the P986T and R1753K mutations
111 were combined, synthetic lethality was still observed with *fyv6Δ* (**Fig. 2B**). These results are
112 consistent with Fyv6 acting to promote the 2nd step of splicing and its deletion, *fyv6Δ*, promoting
113 the 1st step. Combining *fyv6Δ* with a 1st-step Prp8 allele can be synthetically lethal due to failure
114 to properly transition to the 2nd step, while combining *fyv6Δ* with a 2nd-step allele may improve
115 yeast growth by facilitating proper 1st-step/2nd-step equilibrium.

116 **Genetic Interactions between Fyv6 and Prp16 or Prp22**

117 Prp8 1st and 2nd-step alleles, as well as 1st and 2nd-step alleles in U6 snRNA and Cef1, can
118 also genetically interact with mutants of the Prp16 or Prp22 ATPases that promote the 1st to 2nd-
119 step transition or exit out of the 2nd-step by product release, respectively (**Fig. 2A**) (Query and
120 Konarska, 2006, 2012; Eysmont et al., 2019). Based on these observations, we next tested
121 genetic interactions between *fyv6Δ* and Prp16 and Prp22 mutants that presumably slow these
122 conformational changes. Prp16^{R686I} likely slows the 1st-to-2nd-step transition, leads to a *cs*
123 phenotype at 16°C (Hotz and Schwer, 1998), and is synthetically lethal with 1st-step Prp8 alleles
124 (Query and Konarska, 2006). A yeast strain with *fyv6Δ* plus Prp16^{R686I} exacerbates the cold
125 sensitivity, resulting in almost no growth at 16°C and reduced growth at 23°C compared to strains
126 with either allele alone (**Fig. 2D**). The combination of Prp16^{R686I} with *fyv6Δ* also results in reduced
127 growth at 30°C and is synthetic lethal at 37°C. Both *fyv6Δ* and 1st-step Prp8 alleles interact
128 negatively with the Prp16^{R686I} ATPase.

129 The Prp22^{T637A} mutant uncouples ATP hydrolysis from RNA unwinding (Schwer and
130 Meszaros, 2000), likely perturbing the transition out of the 2nd-step conformation and product
131 release. Prp22^{T637A} is also a *cs* allele and does not grow at 16 or 23°C (Schwer and Meszaros,
132 2000 and **Fig. 2E**) and is synthetically lethal with 2nd-step alleles of Cef1 (Query and Konarska,
133 2012). When Prp22^{T637A} and *fyv6Δ* were combined, we did not observe any suppression of the *cs*
134 phenotype of Prp22^{T637A} or the *cs/ts* phenotype of *fyv6Δ* (**Fig. 2E**). Prp22^{T637A}/*fyv6Δ* yeast were
135 viable at 30°C but grew more slowly than strains containing only a single allele. Deletion of *FYV6*
136 results in more pronounced genetic interactions with Prp16^{R686I} than with Prp22^{T637A}, consistent
137 with the deletion acting as a 1st-step allele.

138 **Impact of *fyv6Δ* on Yeast Growth using the ACT1-CUP1 Splicing Reporter Assay**

139 If Fyv6 is a component of the splicing machinery as the genetic interactions suggest, we
140 would also predict changes in *in vivo* splicing in the absence of the protein. To test this, we used
141 the ACT1-CUP1 reporter assay in which changes in the splicing of the reporter pre-mRNA (**Fig.**
142 **3A**) confer proportional changes in the copper tolerance of a sensitized yeast strain with increased
143 splicing efficiency leading to growth at higher copper concentrations (Lesser and Guthrie 1993).
144 Since yeast lacking Fyv6 grow more slowly than WT even under optimal growth conditions (**Fig.**
145 **2**, for example) we scored WT yeast growth on Cu²⁺-containing plates after 48h but *fyv6Δ* yeast
146 were scored after 72h. Consistent with the slow growth and with a function of Fyv6 during splicing,
147 we observed slightly reduced copper tolerance for even the WT ACT1-CUP1 reporter in the *fyv6Δ*
148 strain (**Fig. 3B, C**).

149 We also tested several ACT1-CUP1 reporters containing substitutions in the 5' (U2A,
150 A3C, and A3U) or 3' SS (UuG and gAG) or the BS (A258U, BSG, and BSC, **Fig 3A**) to determine
151 if loss of Fyv6 is especially detrimental or beneficial to introns with nonconsensus sequences.
152 Copper tolerance was similar between WT and *fyv6Δ* yeast containing reporters with the U2A,
153 A3C, UuG, A258U, and BSC substitutions. However, *fyv6Δ* strains containing A3U, BSG, and

154 gAG reporters exhibited less tolerance to copper than WT (**Fig. 3B, C**), suggesting poorer splicing
155 of pre-mRNAs with these substitutions. Previous work has shown that 1st-step alleles of Prp8
156 result in reduced copper tolerance and few ligated mRNA products with the U2A, A3C, BSC, BSG,
157 UuG, and gAG reporters and that 2nd step alleles of Prp8 or Cef1 improve copper tolerance of
158 yeast with the U2A, BSC, BSG, UuG, and gAG reporters (Liu L. et al., 2007; Query and Konarska,
159 2012). Several of these reporters are also limiting for the exon ligation reaction itself (U2A, A3C,
160 BSG, UuG, and gAG; Liu L. et al., 2007). Loss of Fyv6 results in changes in copper tolerance
161 most similar to 1st-step alleles of Prp8 and is consistent with Fyv6 supporting the 2nd step when
162 present.

163 **FYV6Δ Changes 3' SS Selection in an ACT1-CUP1 Splicing Reporter**

164 Finally, since both Prp18 and Slu7 can change 3' SS selection (Kawashima et al., 2009,
165 2014; Frank and Guthrie, 1992), we tested whether or not loss of Fyv6 can also change splicing
166 outcomes. We utilized an ACT1-CUP1 reporter containing an additional, alternative 3' SS
167 proximal to the BS which results in a frameshift when used instead of the distal 3' SS (**Fig. 4A**).
168 Previous studies with this reporter showed that use of the proximal 3' SS greatly increases in the
169 presence of the *slu7-1* allele with an ~20-fold change in the ratio of mRNAs produced using the
170 proximal vs. distal sites (Frank and Guthrie, 1992). Indeed, when this reporter was used, we
171 observed the largest differences in copper tolerance (**Fig. 4B**). To confirm that this change in
172 survival was due to a change in 3' SS usage and use of the proximal SS, we isolated RNAs from
173 the yeast strains and quantified SS usage by primer extension. These results showed an increase
174 in use of the proximal SS and an ~5-fold increase in the ratio of mRNAs produced using the
175 proximal vs. distal sites (**Fig. 4C, D**). Like mutations in Slu7 or loss of Prp18, loss of Fyv6 can
176 also change 3' SS selection and is consistent with function as a 2nd-step splicing factor. These
177 data suggest that Fyv6, like Slu7, helps to enforce a preference for BS distal 3' SS presumably
178 by facilitating docking of the distal SS and/or preventing docking of the proximal site (Fica et al.,
179 2017).

180 **Conclusion**

181 Together the genetic and biochemical data presented here as well as the mass
182 spectrometry and cryo-EM work of others indicate that yeast Fyv6 is a 2nd-step splicing factor and
183 likely is a component of the spliceosome. Our results do not, however, confirm that the unassigned
184 EM density present in yeast C* and P complex spliceosome cryo-EM maps is due to Fyv6. Further
185 work will be needed to confirm that this is indeed the case either through obtaining higher
186 resolution cryo-EM data or experimental approaches that probe protein-protein interactions to
187 map the Fyv6 binding site.

188 Many outstanding questions remain about Fyv6 function. We do not know when Fyv6
189 associates or dissociates from the spliceosome or exactly how it is promoting exon ligation. One
190 possible mechanism could be by direct modulation of Prp22 activity. Several other DExD/H-box
191 ATPases involved in splicing use protein cofactors to stimulate their activity and regulate their
192 association with the spliceosome: Spp2 interacts with the Prp2 ATPase during activation and Ntr1
193 interacts with the Prp43 ATPase during spliceosome disassembly (Tanaka et al., 2007; Silverman
194 et al., 2004; Warkocki et al., 2015). Fyv6 or human FAM192A could allosterically regulate Prp22
195 activity by directly interacting with the protein or by helping it be recruited to the correct
196 spliceosomal complex and RNA substrate. Finally, since it seems likely that Fyv6 is the functional
197 yeast homolog of human FAM192A in terms of pre-mRNA splicing, it will be worth investigating if
198 other functions of FAM192A/Fyv6 are conserved in yeast. FAM192A also associates with the 20S
199 proteasome via interaction with PA28 γ , a 20S proteasome regulator, for ubiquitin-independent
200 protein degradation within the nucleus (Jonik-Nowak et al., 2018). While yeast lack an apparent
201 homolog for PA28 γ (Jonik-Nowak et al., 2018), it may be interesting to determine if Fyv6 is also
202 involved in protein degradation and if there are any Fyv6-dependent links between proteostasis
203 and pre-mRNA splicing.

204 **SUPPLEMENTAL MATERIAL**

205 Supplemental material is available for this article.

206 **ACKNOWLEDGEMENTS**

207 We thank Guillaume Chanfreau and his laboratory for helpful discussions and critical
208 review of the manuscript. We thank Peter Ducos and Tim Grant for assistance in making Figure
209 1.

210 **FUNDING**

211 This work was supported by grants from the National Institutes of Health (R35 GM136261
212 to AAH) and NIH Biotechnology Training Program (T32 GM135066) and National Science
213 Foundation Graduate Research Fellowship Program (Grant No. DGE-1747503) fellowships to
214 KAS.

215 **COMPETING INTERESTS**

216 AAH is a member of the scientific advisory board and carrying out sponsored research for
217 Remix Therapeutics.

218 **METHODS**

219 Yeast strains and plasmids used in this study are described in **Tables S1** and **S2**. Yeast
220 transformation, plasmid shuffling/5-FOA selection, and growth were carried out using standard
221 techniques and media (Trecu and Lundblad 1993; Sikorski and Boeke 1991).

222 **FYV6 deletion**

223 The FYV6 gene was deleted through replacement with a hygromycin resistance cassette
224 by homologous recombination (see **Table S1**; Goldstein and McCusker, 1999). Gene deletion
225 was confirmed by genomic DNA extraction from the strains and PCR amplification of the FYV6
226 genomic locus using primers Fyv6-check-fwd 5'-TGGATCGAACACAGGACCTC-3' and Fyv6-
227 check-rev 5'-GTGGAACGAGCAATCAATGTGATC-3'.

228 **ACT1-CUP1 copper tolerance assays**

229 Yeast strains expressing ACT1-CUP1 reporters were grown to stationary phase in -Leu
230 DO media to maintain selection for plasmids, diluted to $OD_{600} = 0.5$ in 10% (v/v) glycerol, and
231 spotted onto -Leu DO plates containing 0 to 2.5 mM $CuSO_4$ (Lesser and Guthrie 1993; Carrocci
232 et al., 2018). Plates were scored and imaged after 48 h of growth at 30°C for WT strains and after
233 72 h of growth at 30°C for *fyv6Δ* strains due to differential growth between strains.

234 **Growth assays**

235 For temperature-dependent growth assays, yeast strains were grown overnight to
236 stationary phase in YPD media, diluted to $OD_{600} = 0.5$ in 10% (v/v) glycerol, and stamped onto
237 YPD plates. The plates were incubated at 16, 23, 30, or 37°C for the number of days indicated in
238 each figure legend before imaging.

239 For growth assays in the presence of 5-FOA, yeast strains were grown overnight to
240 stationary phase in -Trp DO media, diluted to $OD_{600} = 0.5$ in 10% (v/v) glycerol, and stamped onto
241 -Trp and -Trp +5-FOA plates. The plates were incubated at 30°C for 3 days before imaging.

242 **Primer extension**

243 Cell cultures were inoculated from stationary phase saturated cultures grown overnight in
244 -Leu DO media. The cultures were then grown until $OD_{600} = 0.6 - 0.8$, and $10 OD_{600}$ units were
245 collected by centrifugation. Total RNA was isolated from yeast and contaminating DNA was
246 depleted using the MasterPure Yeast RNA Purification Kit (Epicentre, Madison, WI) protocol with
247 minor changes as previously described (Carrocci et al., 2017). IR700 dye conjugated probes
248 (Integrated DNA Technologies, Skokie, IL) were used for primer extension of the ACT1-CUP1
249 reporter (10 pmol yAC6: /5IRD700/GGCACTCATGACCTTC) and U6 snRNA (2 pmol yU6:
250 /5IRD700/GAACTGCTGATCATGTCTG) (Carrocci et al., 2017; van der Feltz et al., 2021). Primer
251 extension products were visualized on a 7% (w/v) denaturing polyacrylamide gel (42 cm x 22 cm
252 x 0.75 mm) run at 35W for 80 min at RT. Gels were imaged with an Amersham Typhoon NIR
253 laser scanner (Cytiva), and band intensities were quantified with Image J (version 1.53v, 2022).

254 **Network analysis of potential Fyv6 interactions**

255 Protein-protein and protein-RNA interactions found in the atomic model for the P complex
256 spliceosome (6BK8) were identified using LouiseNET and the resulting nodes and edges were
257 plotted as an undirected network model using GEPHI as previously described (Bastian et al.,
258 2009; Kaur et al., 2022).

259 **REFERENCES**

- 260 Auesukaree C, Damnernsawad A, Kruatrachue M, Pokethitiyook P, Boonchird C, Kaneko Y,
261 Harashima S. 2009. Genome-wide identification of genes involved in tolerance to various
262 environmental stresses in *Saccharomyces cerevisiae*. *J Appl Genet* **50**, 301–310.
263 doi:10.1007/BF03195688
- 264 Bastian M, Heymann S, Jacomy M. 2009. Gephi: An Open Source Software for Exploring and
265 Manipulating Networks. *Proceedings of the International AAAI Conference on Web and*
266 *Social Media* **3**, 361–362. doi:10.1609/icwsm.v3i1.13937
- 267 Carrocci TJ, Paulson JC, Hoskins AA. 2018. Functional analysis of Hsh155/SF3b1 interactions
268 with the U2 snRNA/branch site duplex. *RNA* **24**, 1028–1040. doi:10.1261/rna.065664.118
- 269 Carrocci TJ, Zoerner DM, Paulson JC, Hoskins AA. 2017. SF3b1 mutations associated with
270 myelodysplastic syndromes alter the fidelity of branchsite selection in yeast. *Nucleic Acids*
271 *Res* **45**, 4837–4852. doi:10.1093/nar/gkw1349
- 272 Chiu Y-F, Liu Y-C, Chiang T-W, Yeh T-C, Tseng C-K, Wu N-Y, Cheng S-C. 2009. Cwc25 Is a
273 Novel Splicing Factor Required after Prp2 and Yju2 to Facilitate the First Catalytic
274 Reaction. *Mol Cell Biol* **29**, 5671–5678. doi:10.1128/MCB.00773-09
- 275 Eysmont K, Matylla-Kulińska K, Jaskulska A, Magnus M, Konarska MM. 2019. Rearrangements
276 within the U6 snRNA Core during the Transition between the Two Catalytic Steps of
277 Splicing. *Mol Cell* **75**, 538-548.e3. doi:10.1016/j.molcel.2019.05.018
- 278 Fabrizio P, Dannenberg J, Dube P, Kastner B, Stark H, Urlaub H, Lührmann R. 2009. The
279 Evolutionarily Conserved Core Design of the Catalytic Activation Step of the Yeast
280 Spliceosome. *Mol Cell* **36**, 593–608. doi:10.1016/j.molcel.2009.09.040
- 281 Fica SM, Nagai K, 2017. Cryo-electron microscopy snapshots of the spliceosome: structural
282 insights into a dynamic ribonucleoprotein machine. *Nat Struct Mol Biol* **24**, 791–799.
283 doi:10.1038/nsmb.3463

- 284 Fica SM, Oubridge C, Galej WP, Wilkinson ME, Bai X-C, Newman AJ, Nagai K. 2017. Structure
285 of a spliceosome remodelled for exon ligation. *Nature* **542**, 377–380.
286 doi:10.1038/nature21078
- 287 Frank D, Guthrie C. 1992. An essential splicing factor, SLU7, mediates 3' splice site choice in
288 yeast. *Genes Dev* **6**, 2112–2124. doi:10.1101/gad.6.11.2112
- 289 Goldstein AL, McCusker JH. 1999. Three new dominant drug resistance cassettes for gene
290 disruption in *Saccharomyces cerevisiae*. *Yeast* **15**, 1541–1553. doi:10.1002/(SICI)1097-
291 0061(199910)15:14<1541::AID-YEA476>3.0.CO;2-K
- 292 Hotz H-R, Schwer B. 1998. Mutational Analysis of the Yeast DEAH-Box Splicing Factor Prp16.
293 *Genetics* **149**, 807–815. doi:10.1093/genetics/149.2.807
- 294 Huh W-K, Falvo JV, Gerke LC, Carroll AS, Howson RW, Weissman JS, O'Shea EK. 2003. Global
295 analysis of protein localization in budding yeast. *Nature* **425**, 686–691.
296 doi:10.1038/nature02026
- 297 James S-A, Turner W, Schwer B. 2002. How Slu7 and Prp18 cooperate in the second step of
298 yeast pre-mRNA splicing. *RNA* **8**, 1068–1077. doi:10.1017/s1355838202022033
- 299 Jonik-Nowak B, Menneteau T, Fesquet D, Baldin V, Bonne-Andrea C, Méchali F, Fabre B,
300 Boisguerin P, de Rossi S, Henriquet C, et al. 2018. PIP30/FAM192A is a novel regulator
301 of the nuclear proteasome activator PA28 γ . *Proc. Natl. Acad. Sci. U.S.A.* **115**, E6477-
302 E6486. doi:10.1073/pnas.1722299115
- 303 Jumper J, Evans R, Pritzel A, Green T, Figurnov M, Ronneberger O, Tunyasuvunakool K, Bates
304 R, Žídek A, Potapenko A, et al. 2021. Highly accurate protein structure prediction with
305 AlphaFold. *Nature* **596**, 583–589. doi:10.1038/s41586-021-03819-2
- 306 Kaur H, van der Feltz C, Sun Y, Hoskins AA. 2022. Network theory reveals principles of
307 spliceosome structure and dynamics. *Structure* **30**, 190-200.e2.
308 doi:10.1016/j.str.2021.09.003

- 309 Kawashima T, Douglass S, Gabunilas J, Pellegrini M, Chanfreau GF. 2014. Widespread Use of
310 Non-productive Alternative Splice Sites in *Saccharomyces cerevisiae*. *PLOS Genetics* **10**,
311 e1004249. doi:10.1371/journal.pgen.1004249
- 312 Kawashima T, Pellegrini M, Chanfreau GF. 2009. Nonsense-mediated mRNA decay mutes the
313 splicing defects of spliceosome component mutations. *RNA* **15**, 2236–2247.
314 doi:10.1261/rna.1736809
- 315 Lesser CF, Guthrie C. 1993. Mutational analysis of pre-mRNA splicing in *Saccharomyces*
316 *cerevisiae* using a sensitive new reporter gene, CUP1. *Genetics* **133**, 851–863.
317 doi:10.1093/genetics/133.4.851
- 318 Liu L, Query CC, Konarska MM. 2007. Opposing classes of prp8 alleles modulate the transition
319 between the catalytic steps of pre-mRNA splicing. *Nat Struct Mol Biol* **14**, 519–526.
320 doi:10.1038/nsmb1240
- 321 Liu S, Li X, Zhang L, Jiang J, Hill RC, Cui Y, Hansen KC, Zhou ZH, Zhao R. 2017. Structure of
322 the yeast spliceosomal postcatalytic P complex. *Science* **358**, 1278–1283.
323 doi:10.1126/science.aar3462
- 324 Liu Y-C, Chen H-C, Wu N-Y, Cheng S-C. 2007. A Novel Splicing Factor, Yju2, Is Associated with
325 NTC and Acts after Prp2 in Promoting the First Catalytic Reaction of Pre-mRNA Splicing.
326 *Mol Cell Biol* **27**, 5403–5413. doi:10.1128/MCB.00346-07
- 327 Maitra N, Anandhakumar J, Blank HM, Kaplan CD, Polymenis M. 2019. Perturbations of
328 Transcription and Gene Expression-Associated Processes Alter Distribution of Cell Size
329 Values in *Saccharomyces cerevisiae*. *G3: Genes, Genomes, Genetics* **9**, 239–250.
330 doi:10.1534/g3.118.200854
- 331 Needleman SB, Wunsch CD. 1970. A general method applicable to the search for similarities in
332 the amino acid sequence of two proteins. *Journal of Molecular Biology* **48**, 443–453.
333 doi:10.1016/0022-2836(70)90057-4

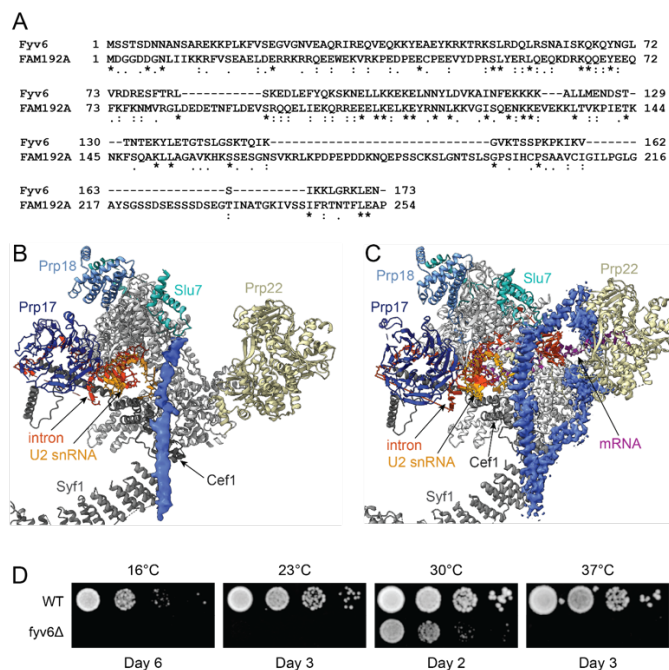
- 334 Ohrt T, Odenwalder P, Dannenberg J, Prior M, Warkocki Z, Schmitzova J, Karaduman R, Gregor
335 I, Enderlein J, Fabrizio P, Luhmann R. 2013. Molecular dissection of step 2 catalysis of
336 yeast pre-mRNA splicing investigated in a purified system. *RNA* **19**, 902–915.
337 doi:10.1261/rna.039024.113
- 338 Page N, Gerard-Vincent M, Menard P, Beaulieu M, Azuma M, Dijkgraaf GJP, Li H, Marcoux J,
339 Nguyen T, Dowse T, Sdicu A-M, Bussey H. 2003. A *Saccharomyces cerevisiae* genome-
340 wide mutant screen for altered sensitivity to K1 killer toxin. *Genetics* **163**, 875–894.
341 doi:10.1093/genetics/163.3.875
- 342 Pettersen EF, Goddard TD, Huang CC, Meng EC, Couch GS, Croll TI, Morris JH, Ferrin TE. 2021.
343 UCSF ChimeraX: Structure visualization for researchers, educators, and developers.
344 *Protein Sci* **30**, 70–82. doi:10.1002/pro.3943
- 345 Plaschka C, Newman AJ, Nagai K. 2019. Structural Basis of Nuclear pre-mRNA Splicing: Lessons
346 from Yeast. *Cold Spring Harb Perspect Biol* **11**, a032391.
347 doi:10.1101/cshperspect.a032391
- 348 Query CC, Konarska MM. 2012. CEF1/CDC5 alleles modulate transitions between catalytic
349 conformations of the spliceosome. *RNA* **18**, 1001–1013. doi:10.1261/rna.029421.111
- 350 Query CC, Konarska MM. 2006. Splicing fidelity revisited. *Nat Struct Mol Biol* **13**, 472–474.
351 doi:10.1038/nsmb0606-472
- 352 Query CC, Konarska MM. 2004. Suppression of Multiple Substrate Mutations by Spliceosomal
353 prp8 Alleles Suggests Functional Correlations with Ribosomal Ambiguity Mutants. *Mol Cell*
354 **14**, 343–354. doi:10.1016/S1097-2765(04)00217-5
- 355 Schneider S, Campodonico E, Schwer B. 2004. Motifs IV and V in the DEAH Box Splicing Factor
356 Prp22 Are Important for RNA Unwinding, and Helicase-defective Prp22 Mutants Are
357 Suppressed by Prp8*. *JBC* **279**, 8617–8626. doi:10.1074/jbc.M312715200
- 358 Schwer B. 2008. A Conformational Rearrangement in the Spliceosome Sets the Stage for Prp22-
359 Dependent mRNA Release. *Mol Cell* **30**, 743–754. doi:10.1016/j.molcel.2008.05.003

- 360 Schwer B, Guthrie C. 1992. A conformational rearrangement in the spliceosome is dependent on
361 PRP16 and ATP hydrolysis. *The EMBO Journal* **11**, 5033–5039. doi:10.1002/j.1460-
362 2075.1992.tb05610.x
- 363 Schwer B, Meszaros T. 2000. RNA helicase dynamics in pre-mRNA splicing. *The EMBO Journal*
364 **19**, 6582–6591. doi:10.1093/emboj/19.23.6582
- 365 Semlow DR, Blanco MR, Walter NG, Staley JP. 2016. Spliceosomal DEAH-Box ATPases
366 Remodel Pre-mRNA to Activate Alternative Splice Sites. *Cell* **164**, 985–998.
367 doi:10.1016/j.cell.2016.01.025
- 368 Sikorski RS, Boeke JD. 1991. In vitro mutagenesis and plasmid shuffling: from cloned gene to
369 mutant yeast. *Methods Enzymol* **194**, 302–318. doi:10.1016/0076-6879(91)94023-6
- 370 Silverman EJ, Maeda A, Wei J, Smith P, Beggs JD, Lin R-J. 2004. Interaction between a G-Patch
371 Protein and a Spliceosomal DEXD/H-Box ATPase That Is Critical for Splicing. *Molecular*
372 *and Cellular Biology* **24**, 10101–10110. doi:10.1128/MCB.24.23.10101-10110.2004
- 373 Tanaka N, Aronova A, Schwer B. 2007. Ntr1 activates the Prp43 helicase to trigger release of
374 lariat-intron from the spliceosome. *Genes Dev* **21**, 2312–2325. doi:10.1101/gad.1580507
- 375 Treco DA, Lundblad V. 1993. Preparation of Yeast Media. *Current Protocols in Molecular Biology*
376 **23**, 13.1.1-13.1.7. doi:10.1002/0471142727.mb1301s23
- 377 Tseng C-K, Liu H-L, Cheng S-C. 2011. DEAH-box ATPase Prp16 has dual roles in remodeling of
378 the spliceosome in catalytic steps. *RNA* **17**, 145–154. doi:10.1261/rna.2459611
- 379 Umen JG, Guthrie C. 1995a. A novel role for a U5 snRNP protein in 3' splice site selection. *Genes*
380 *Dev* **9**, 855–868. doi:10.1101/gad.9.7.855
- 381 Umen JG, Guthrie C. 1995b. Prp16p, Slu7p, and Prp8p interact with the 3' splice site in two
382 distinct stages during the second catalytic step of pre-mRNA splicing. *RNA* **1**, 584–597.
- 383 van der Feltz C, Nikolai B, Schneider C, Paulson JC, Fu X, Hoskins AA. 2021. *Saccharomyces*
384 *cerevisiae* Ecm2 modulates the catalytic steps of pre-mRNA splicing. *RNA* **27**, 591–603.
385 doi:10.1261/rna.077727.120

- 386 Viladevall L, Serrano R, Ruiz A, Domenech G, Giraldo J, Barceló A, Ariño J. 2004.
387 Characterization of the calcium-mediated response to alkaline stress in *Saccharomyces*
388 *cerevisiae*. *J Biol Chem* **279**, 43614–43624. doi:10.1074/jbc.M403606200
- 389 Villa T, Guthrie C. 2005. The Isy1p component of the NineTeen Complex interacts with the
390 ATPase Prp16p to regulate the fidelity of pre-mRNA splicing. *Genes Dev* **19**, 1894–1904.
391 doi:10.1101/gad.1336305
- 392 Wagner JDO, Jankowsky E, Company M, Pyle AM, Abelson JN. 1998. The DEAH-box protein
393 PRP22 is an ATPase that mediates ATP-dependent mRNA release from the spliceosome
394 and unwinds RNA duplexes. *The EMBO Journal* **17**, 2926–2937.
395 doi:10.1093/emboj/17.10.2926
- 396 Wan R, Bai R, Yan C, Lei J, Shi Y. 2019. Structures of the Catalytically Activated Yeast
397 Spliceosome Reveal the Mechanism of Branching. *Cell* **177**, 339-351.e13.
398 doi:10.1016/j.cell.2019.02.006
- 399 Warkocki Z, Odenwälder P, Schmitzová J, Platzmann F, Stark H, Urlaub H, Ficner R, Fabrizio P,
400 Lührmann R. 2009. Reconstitution of both steps of *Saccharomyces cerevisiae* splicing
401 with purified spliceosomal components. *Nat Struct Mol Biol* **16**, 1237–1243.
402 doi:10.1038/nsmb.1729
- 403 Warkocki Z, Schneider C, Mozaffari-Jovin S, Schmitzová J, Höbartner C, Fabrizio P, Lührmann
404 R. 2015. The G-patch protein Spp2 couples the spliceosome-stimulated ATPase activity
405 of the DEAH-box protein Prp2 to catalytic activation of the spliceosome. *Genes Dev* **29**,
406 94–107. doi:10.1101/gad.253070.114
- 407 Wilkinson ME, Fica SM, Galej WP, Nagai K. 2021. Structural basis for conformational equilibrium
408 of the catalytic spliceosome. *Mol Cell* **81**, 1439-1452.e9. doi:10.1016/j.molcel.2021.02.021
- 409 Wilson TE. 2002. A Genomics-Based Screen for Yeast Mutants with an Altered
410 Recombination/End-Joining Repair Ratio. *Genetics* **162**, 677–688.
411 doi:10.1093/genetics/162.2.677

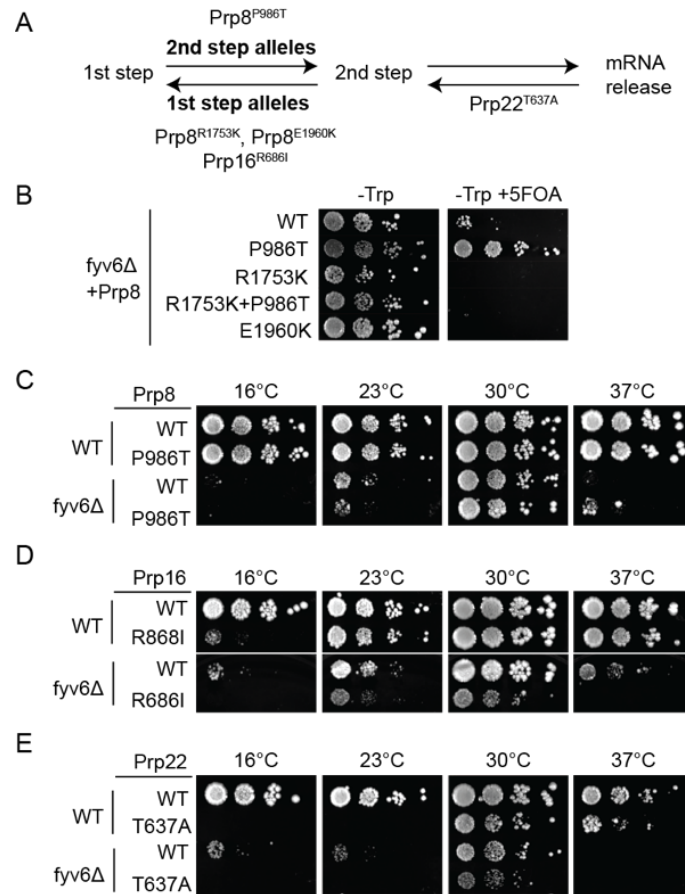
- 412 Yan C, Wan R, Bai R, Huang G, Shi Y. 2017. Structure of a yeast step II catalytically activated
413 spliceosome. *Science* **355**, 149–155. doi:10.1126/science.aak9979
- 414 Zhan X, Lu Y, Zhang X, Yan C, Shi Y. 2022. Mechanism of exon ligation by human spliceosome.
415 *Mol Cell* **82**, 2769-2778.e4. doi:10.1016/j.molcel.2022.05.021

416 **FIGURES**



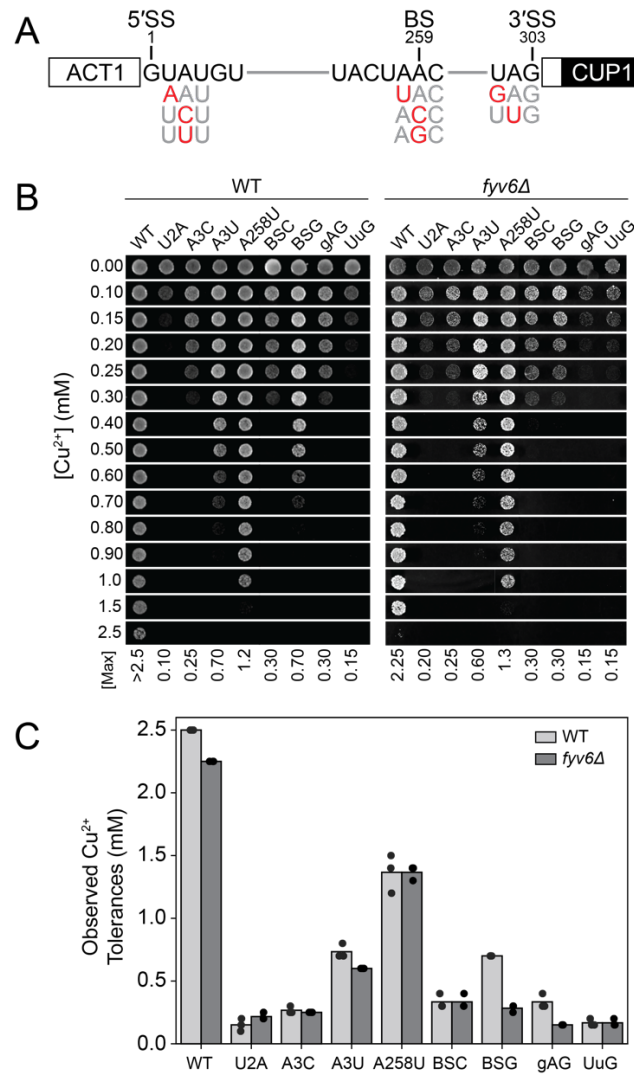
417

418 **Figure 1. Sequence Alignment of Fyv6 with FAM192 and Unassigned EM Density in Yeast**
 419 **Spliceosome Structures.** **A)** Sequence based alignment of *S. cerevisiae* Fyv6 and human
 420 FAM192A using EMBOSS Needle (Needleman and Wunsch, 1970). **B), C)** Superposition of the
 421 atomic models for the spliceosome C* (panel B, 5MQ0) and P (panel C, 6BK8) complexes with
 422 the unassigned EM density shown in blue spacefill. Images were prepared using ChimeraX
 423 (Pettersen et al., 2021). **D)** Impact of *fyv6Δ* on yeast growth at various temperatures. Plates were
 424 imaged on the days shown.
 425



426
427

Figure 2. Genetic interactions between Fyv6 and Prp8, Prp16, or Prp22. **A)** Diagram of how Prp8, Prp16, and Prp22 alleles impact the 1st and 2nd steps of splicing. **B)** Alleles of Prp8 were combined with *fyv6Δ* in Prp8 shuffle strains and grown on -Trp or -Trp+5-FOA plates. Yeast growth was imaged after 3 days at 30°C. **C)** Prp8^{P986T}/*fyv6Δ* strains were tested for suppression or exacerbation of temperature-dependent growth phenotypes. **D, E)** Alleles of Prp16 and Prp22 were combined with *fyv6Δ* and tested for suppression or exacerbation of temperature-dependent growth phenotypes. For panels C-E, yeast were plated on YPD and imaged after 3 (30°C), 4 (23°C and 37°C), or 10 (16°C) days.

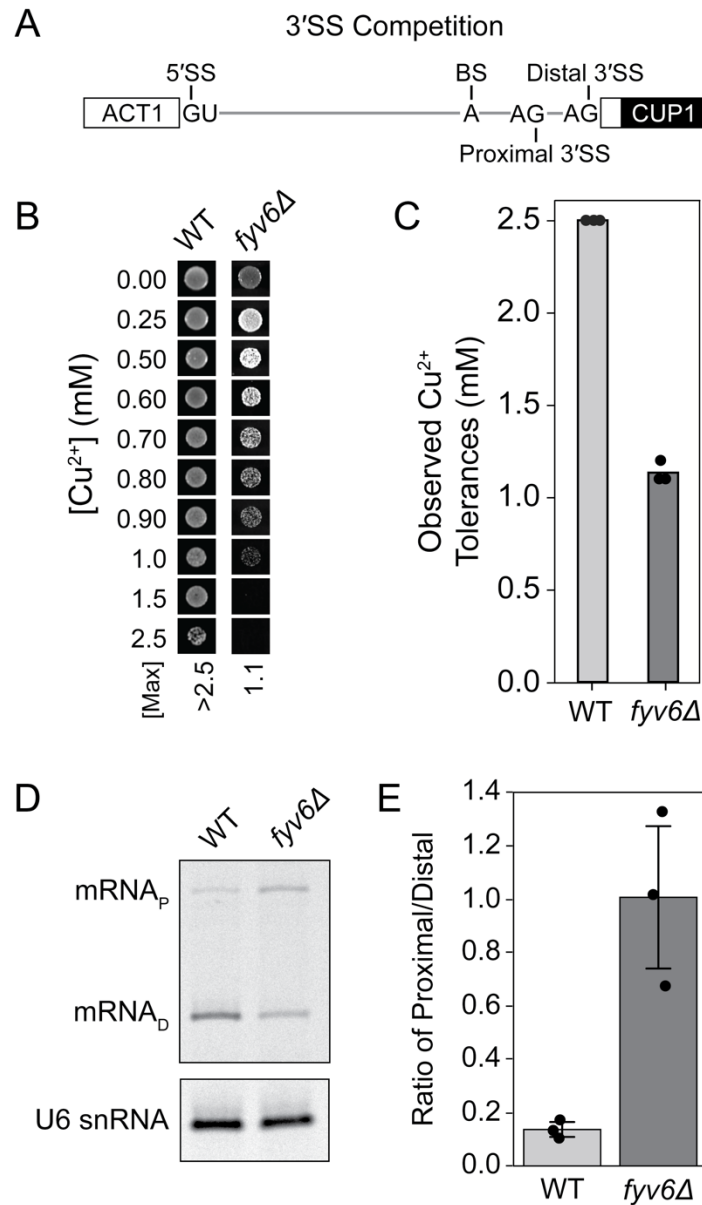


436

437 **Figure 3. Impact of FYV6 deletion on yeast copper tolerance using the ACT1-CUP1 assay.**

438 **A)** Schematic of the WT ACT1-CUP1 reporter along with intronic substitutions. **B)** Images of
 439 representative yeast growth on copper containing media shown after 48 (WT) or 72 h (*fyv6Δ*) for
 440 strains containing the indicated ACT1-CUP1 reporters. **C)** Maximum copper tolerances observed
 441 for each strain for *N*=3 replicates (dots). Bars represent the average values.
 442

443

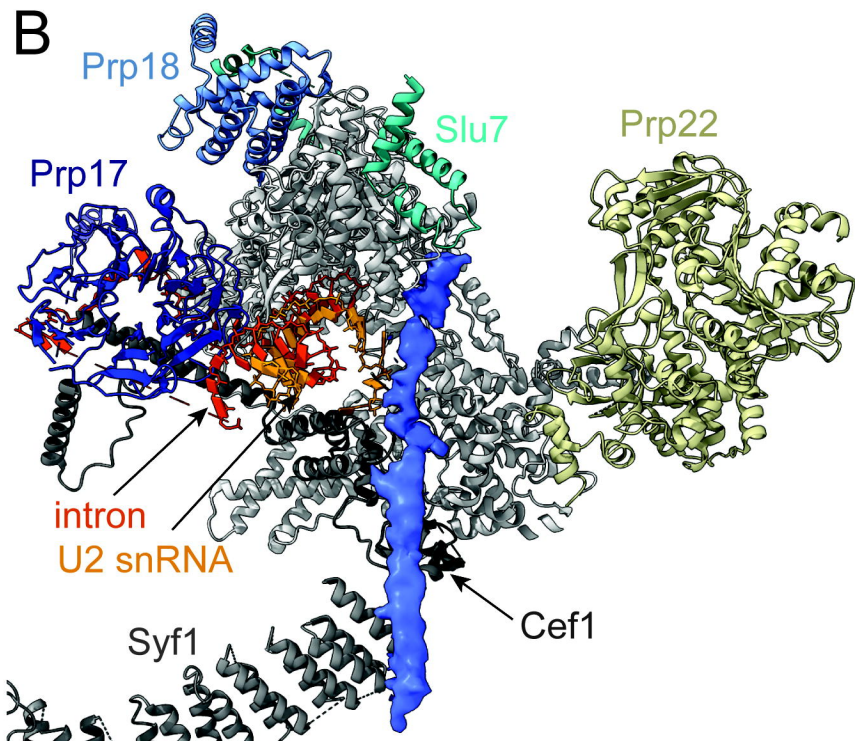
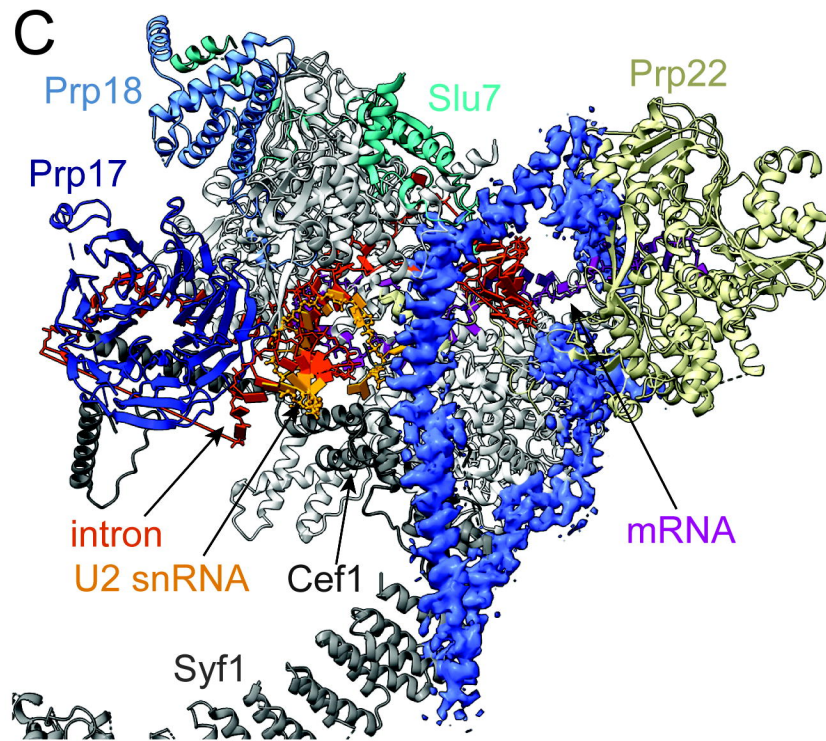
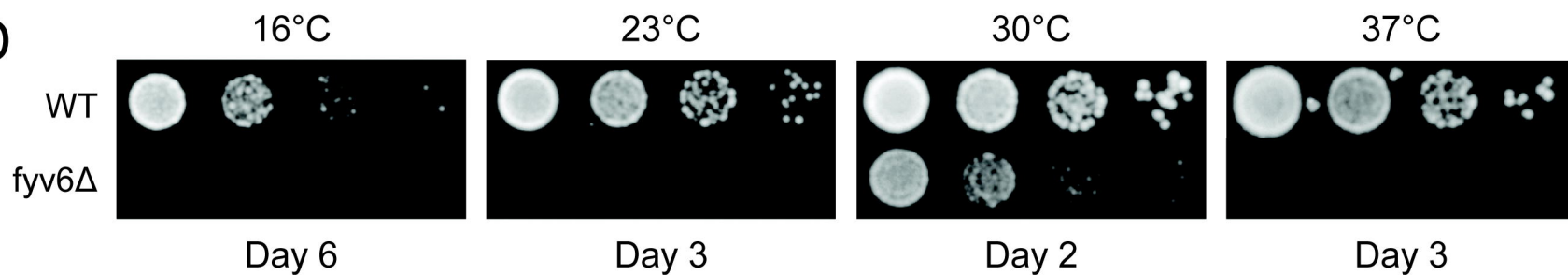


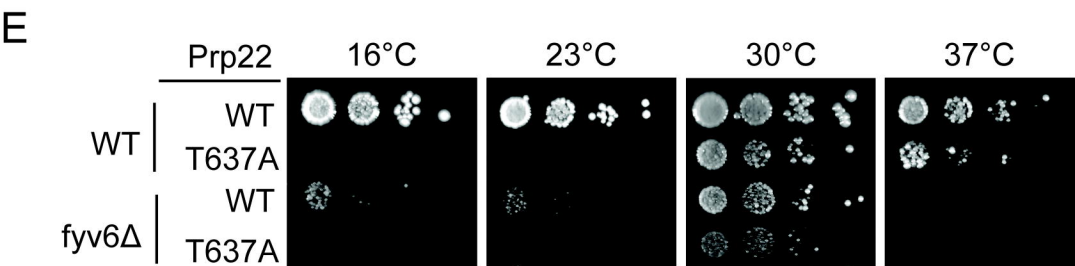
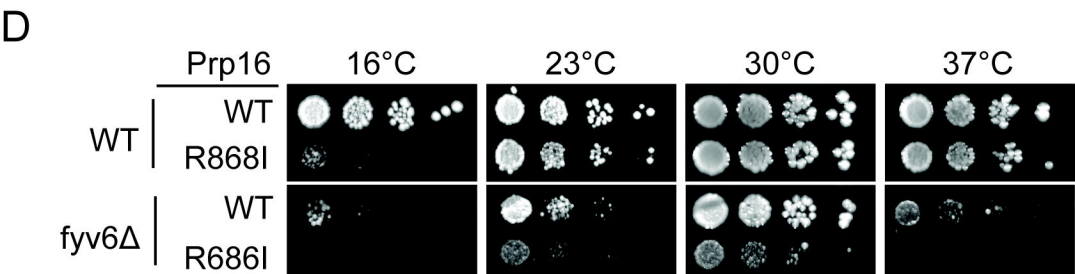
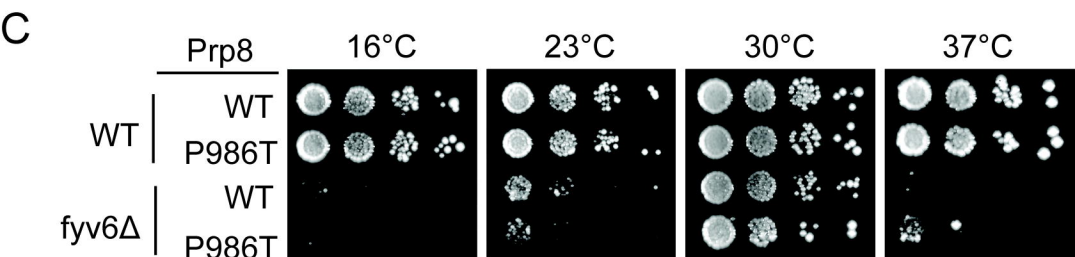
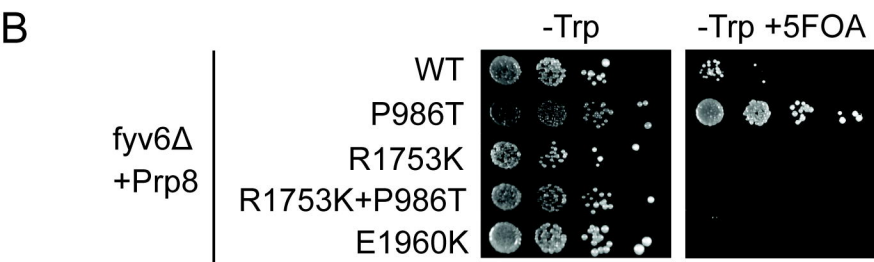
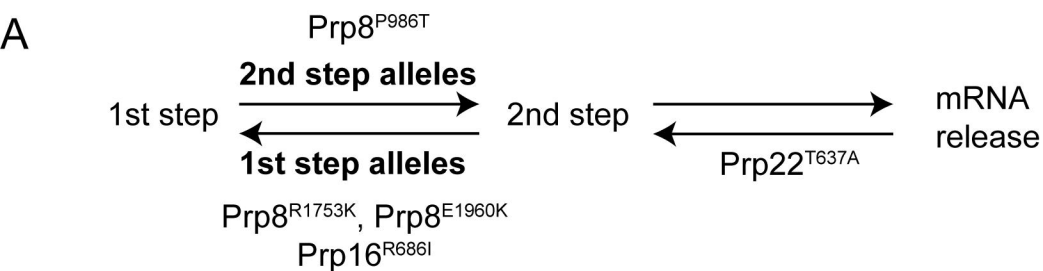
444

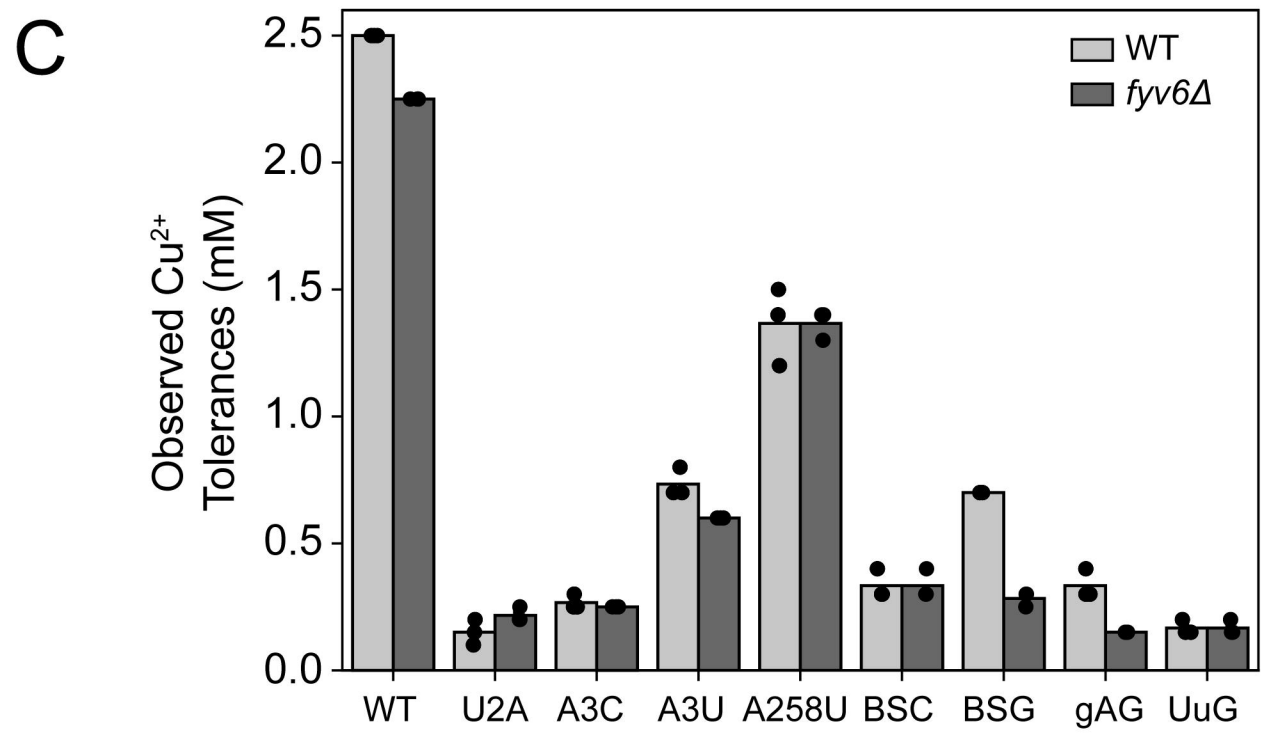
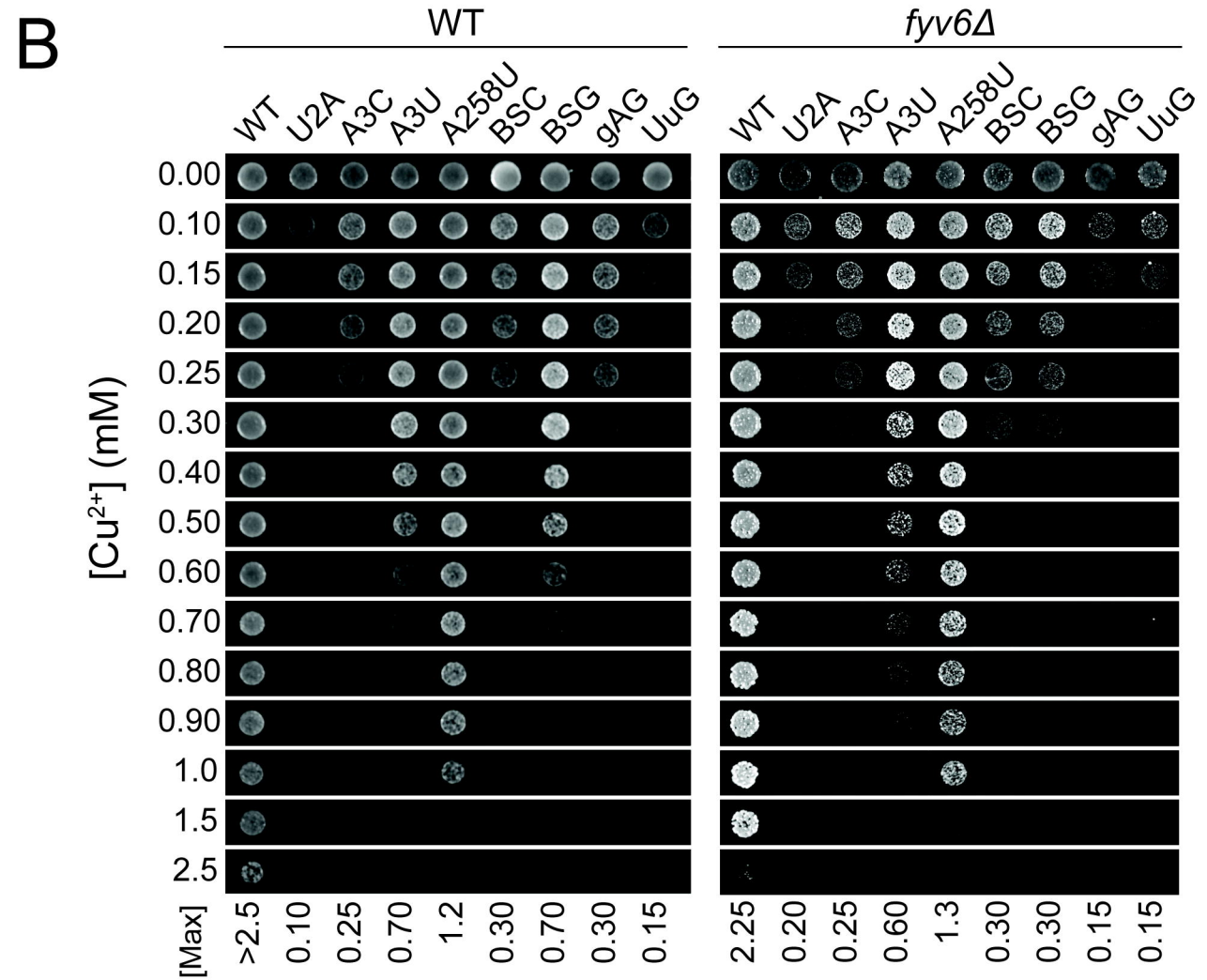
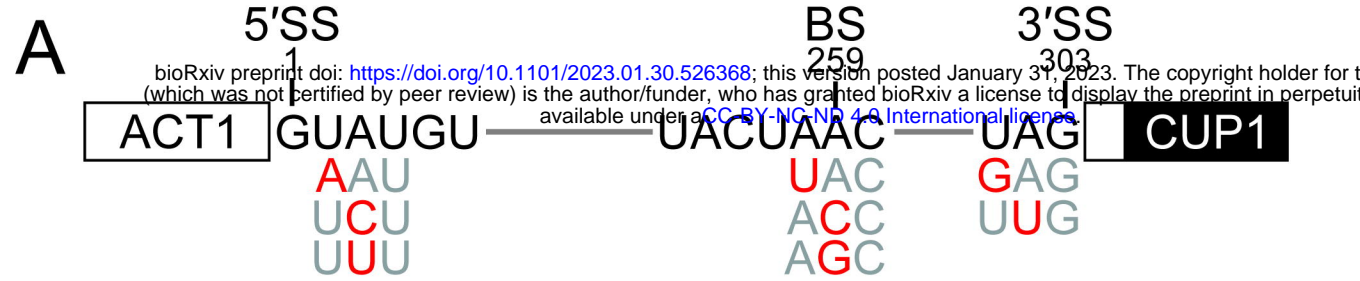
445 **Figure 4. Loss of Fyv6 Changes 3' SS Selection in Yeast.** **A)** Schematic of the 3' SS
 446 competition reporter (3' SS comp) showing relative locations of the proximal and distal sites. **B)**
 447 Images of representative yeast growth on copper containing media shown after 48 (WT) or 72 h
 448 (*fyv6Δ*) for strains containing the 3' SS comp ACT1_CUP1 reporter. **C)** Maximum copper
 449 tolerances observed for each strain for $N=3$ replicates (dots). Bars represent the average values.
 450 **D)** Representative primer extension analysis of mRNAs generated by yeast using the distal
 451 ($mRNA_D$) or proximal ($mRNA_P$) 3' SS in the presence (WT) or absence of Fyv6 (*fyv6Δ*). U6 snRNA
 452 was analyzed as a loading control. **E)** Quantification of the primer extension results from $N=3$
 453 replicates (dots) expressed as a ratio of $mRNA_P/mRNA_D$. Bars represent the average of the
 454 replicates \pm SD. Means between two experimental groups were compared with an unpaired
 455 student's t-test of equal variance ($p = 0.01014$).

A

Fyv6	1	MSSTSDNNANSAREKKPLKFVSEGVGNVEAQRIREQVEQKKYEA EYKRKTRKSLRDQLRSNAISKQKQYNGL	72
FAM192A	1	MDGGDDGNLI IKKRFVSEAELDERRKRRQEEWEKVRKPEDPEECPEEVYDPRSLYERLQE QKDRKQOEYEEQ	72
		...* * : : : : : : : : : : : : * : : ** :*: : : * :*: :*	
Fyv6	73	VRDRESFTRL-----SKEDLEFYQKSKNELLKKEKELNNYLDVKAINFEK KKK---ALLMENDST-	129
FAM192A	73	FKFKNMVRGLDEDETNFLDEVSRQOELIEKQRREEELKELKEYRNNLKKVGISQENKKEVEK KLTVKPIETK	144
		:: : : . * * :*: : : : : : * ** : ** . * * . . * . * :*: : * : : . *	
Fyv6	130	--TNTEKYLETGTSLGSKTQIK-----GVKTSSPKPKIKV-----	162
FAM192A	145	NKFSQAKLLAGAVKHKSSSESGNSVKRLKPDPEPDDKNQEPSSCKSLGNTSLSGPSIHCPSAAVCIGILPGLG	216
		. * * . . . * . . : : : : : * . . * . . : : : : :	
Fyv6	163	-----S-----IKKLGRKLEN-	173
FAM192A	217	AYSGSSDSESSSDSEGTINATGKIVSSIFRTNTFLEAP	254
		: : : : : * : . **	

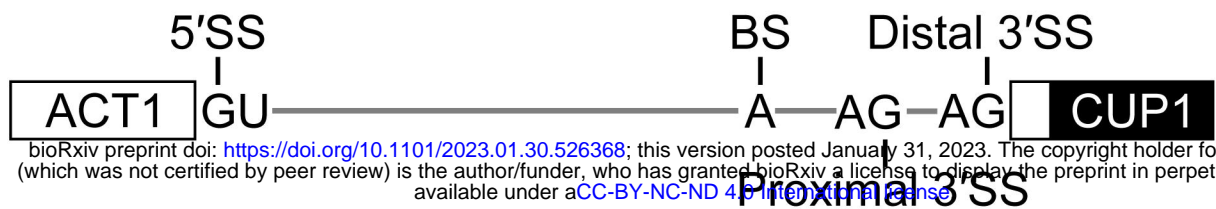
B**C****D**



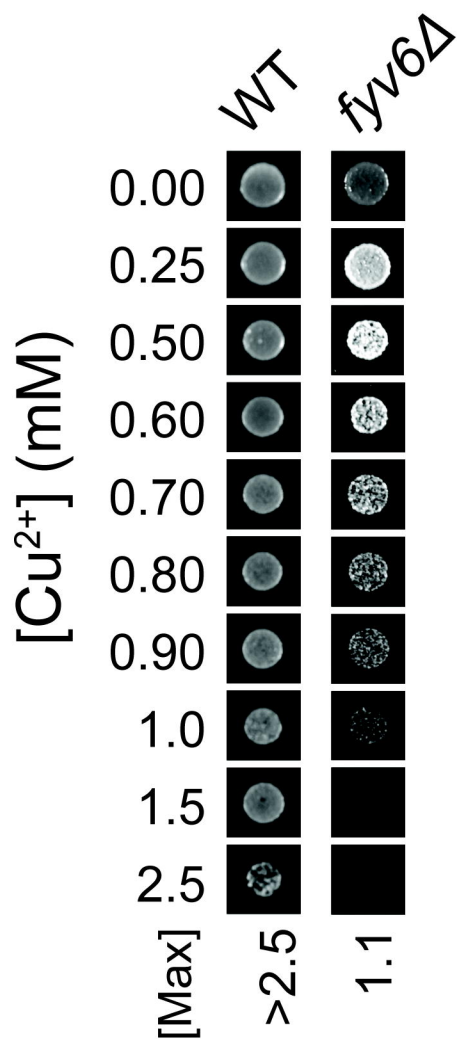


A

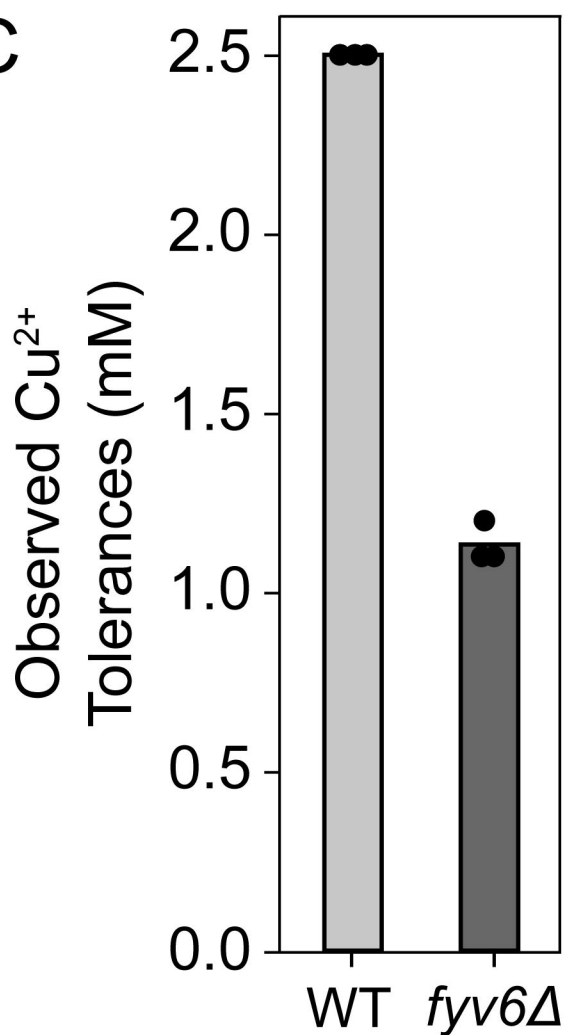
3'SS Competition



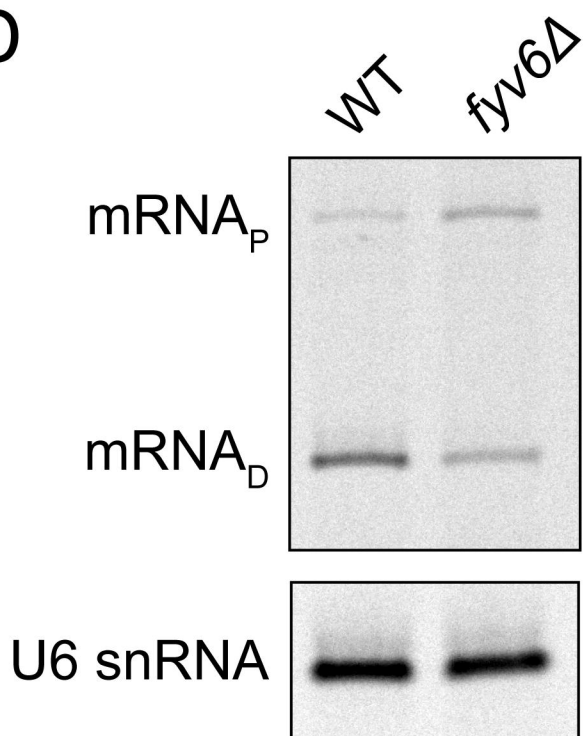
B



C



D



E

